Supplement of Earth Syst. Dynam., 16, 1135–1151, 2025
https://doi.org/10.5194/esd-16-1135-2025-supplement

Earth System Dynamics
Open Access
EGU

Supplement of

Future changes in regional inter-monthly precipitation patterns of the East Asian summer monsoon and associated uncertainty factors

Yeon-Hee Kim and Seung-Ki Min

Correspondence to: Seung-Ki Min (skmin@postech.ac.kr)

Table S1. List of CMIP6 models used in this study

Model	Institution	Resolution (Long. × Lat.)
ACCESS-CM2	Commonwealth Scientific and Industrial Research Organisation and Australian Research Council Centre of Excellence for Climate System Science, Australia	192 × 144
ACCESS-ESM1-5		192 × 145
BCC-CSM2-MR	Beijing Climate Center, China Meteorological Administration, China	320 × 160
CanESM5	Canadian Centre for Climate Modelling and Analysis, Canada	128 × 64
CESM2	National Center for Atmospheric Research	288 × 192
CESM2-WACCM		288 × 192
CMCC-CM2-SR5	Fondazione Centro Euro-Mediterraneo sui Cambiamenti Climatici	288 × 192
CNRM-CM6-1	Centre National de Recherches Météorologiques, Météo-France, France	256 × 128
CNRM-ESM2-1		256 × 128
EC-Earth3	EC-Earth-Consortium	512 × 256
EC-Earth3-Veg		512 × 256
FGOALS-g3	Chinese Academy of Sciences, China	180 × 80
GFDL-ESM4	Geophysical Fluid Dynamics Laboratory, USA	288 × 180
INM-CM4-8	Institute for Numerical Mathematics, Russia	180 × 120
INM-CM5-0		180 × 120
IPSL-CM6A-LR	Institut Pierre-Simon Laplace, France	144 × 143
KACE-1-0-G	National Institute of Meteorological Science/Korea Meteorological Administration, Korea	192 × 144
MIROC6	Atmosphere and Ocean Research Institute (AORI), National Institute for Environmental Studies (NIES), Japan Agency for Marine-Earth Science and Technology (JAMSTEC), RIKEN Center for Computational Science (R-CCS), Japan	256 × 128
MIROC-ES2L		128 × 64
MPI-ESM1-2-HR	Max Planck Institute for Meteorology, Germany	384 × 192
MPI-ESM1-2-LR		192 × 96
MRI-ESM2-0	Meteorological Research Institute, Japan	320 × 160
NorESM2-LM	Norwegian Earth System Model (NorESM) climate modeling Consortium of the Center for International Climate Research (CICERO), Norwegian Meteorological Institute, National Energy Research Scientific Computing Center (NERSC), Norsk Institutt for Luftforskning (NILU), University of Bergen, University of Oslo, and UNI, Norway	144 × 96
NorESM2-MM		288 × 192
UKESM1-0-LL	Met Office Hadley Centre, UK	192 × 144

Table S2. List of CMIP5 models used in this study

Model	Institution	Resolution (Long. × Lat.)
bcc-csm1-1	Beijing Climate Center, China Meteorological Administration, China	128 × 64
bcc-csm1-1-m		320 × 160
BNU-ESM	Beijing Normal University, China	128 × 64
CanESM2	Canadian Centre for Climate Modelling and Analysis, Canada	128 × 64
CCSM4	National Center for Atmospheric Research (NCAR), USA	288 × 192
CNRM-CM5	Centre National de Recherches Météorologiques, Météo-France, France	256 × 128
CSIRO-Mk3-6-0	Australian Commonwealth Scientific and Industrial Research Organization, Australia	192 × 96
FGOALS-g2	Institute of Atmospheric Physics, Chinese Academy of Sciences, China	128 × 60
GFDL-CM3	Geophysical Fluid Dynamics Laboratory, USA	144 × 90
GFDL-ESM2G		144 × 90
GFDL-ESM2M		144 × 90
HadGEM2-AO	Met Office Hadley Centre, UK	192 × 145
HadGEM2-ES		192 × 145
IPSL-CM5A-LR	Institut Pierre-Simon Laplace, France	96 × 96
IPSL-CM5A-MR		144 × 143
MIROC5	Atmosphere and Ocean Research Institute (AORI), National Institute for Environmental Studies (NES), Japan Agency for Marine-Earth Science and Technology (JAMSTEC), Japan	256 × 128
MIROC-ESM		128 × 64
MIROC-ESM-CHEM		128 × 64
MPI-ESM-LR	Max Planck Institute for Meteorology, Germany	192 × 96
MPI-ESM-MR		192 × 96
MRI-CGCM3	Meteorological Research Institute, Japan	320 × 160
NorESM1-M	Norwegian Climate Centre, Norway	144 × 96

Table S3. Relative contribution (RC, %) of internal variability (I), model uncertainty (M), and scenario uncertainty (S) to variance in total projection uncertainty for near-term (NT), mid-term (MT) and long-term (LT) projections of precipitation change over East Asia (EA), China (CHA), Korea (KOR) and Japan (JAP)

Monsoon Rainband Index	Model	RC	EA			CHA			KOR			JAP		
			NT	MT	LT	NT	MT	LT	NT	MT	LT	NT	MT	LT
Northward Migration	CMIP6	M	60.0	70.9	63.8	59.2	66.4	65.5	63.7	69.6	66.8	59.7	68.1	68.1
		S	0.6	0.3	18.8	0.1	0.1	14.0	0.3	1.1	9.7	0.2	0.6	4.5
		I	39.4	28.8	17.4	40.7	33.5	20.6	36.0	29.2	23.6	40.1	31.4	27.5
	CMIP5	M	67.1	72.8	76.7	60.9	73.2	81.4	60.6	73.9	77.1	57.5	68.6	71.4
		S	2.3	3.5	10.8	1.4	1.8	1.2	1.9	1.7	5.2	2.3	4.0	12.2
		I	30.7	23.7	12.5	37.7	25.0	17.4	37.6	24.4	17.7	40.2	27.4	16.4
Peak Time	CMIP6	M	55.7	64.9	74.7	50.7	62.4	72.8	55.7	66.8	74.2	59.8	68.7	81.4
		S	2.0	0.8	4.6	1.0	1.0	2.6	0.2	0.5	3.5	1.7	0.4	1.2
		I	42.3	34.3	20.7	48.3	36.6	24.6	44.0	32.7	22.3	38.5	30.9	17.4
	CMIP5	M	50.4	56.6	63.8	52.8	64.1	78.1	58.4	55.9	67.2	51.6	56.4	65.8
		S	0.5	2.3	13.4	1.3	1.1	2.2	0.4	0.1	5.1	0.2	3.4	11.9
		I	49.1	41.1	22.8	45.9	34.7	19.7	41.2	44.0	27.7	48.3	40.2	22.4

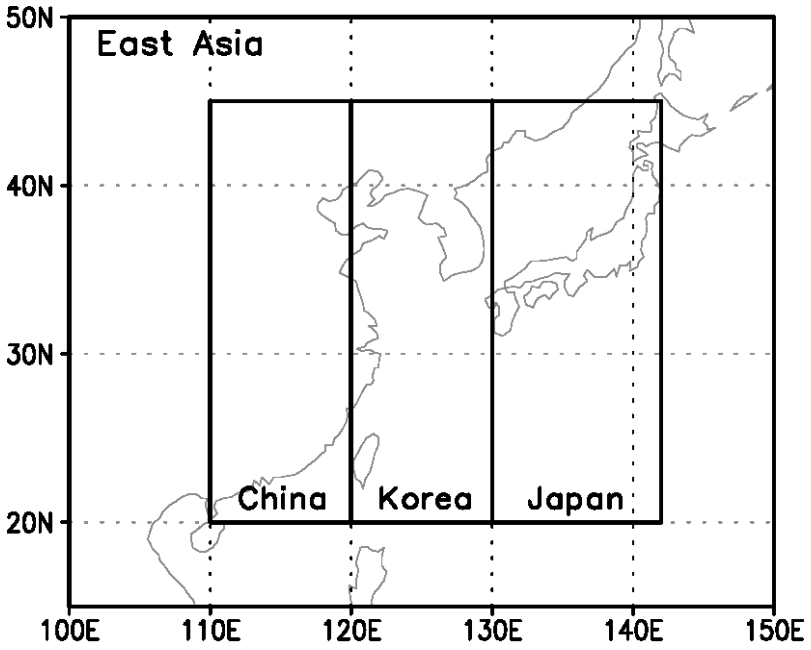

Figure S1. Geographical location of the East Asian domain and three subregions—China, Korea, and Japan—analyzed in this study

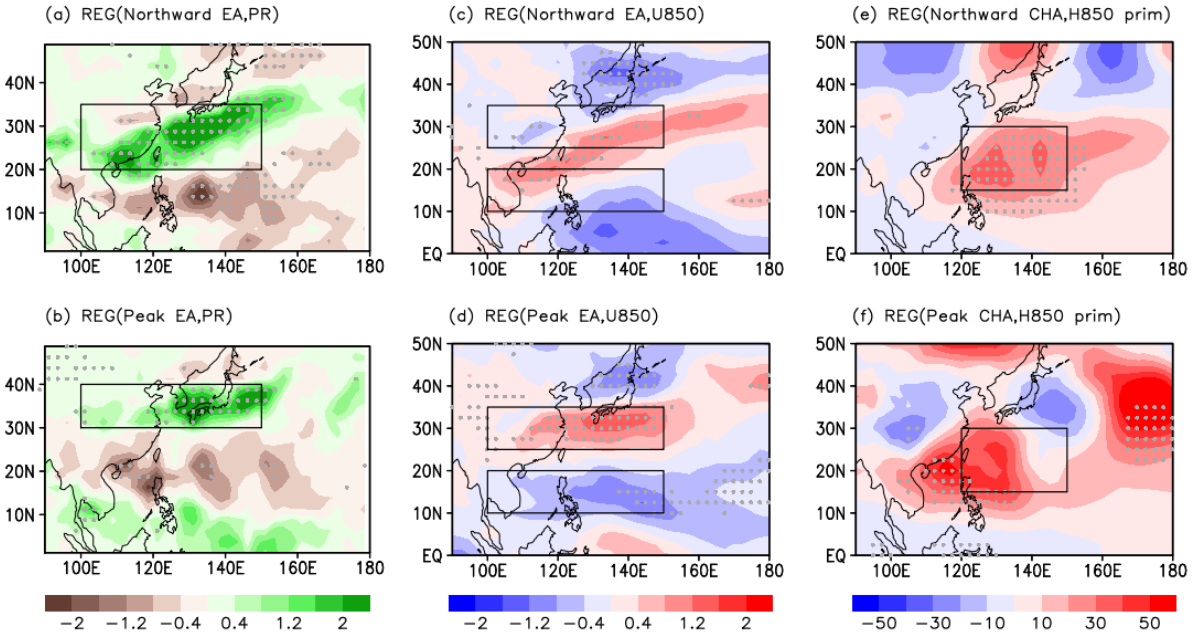

Figure S2. Regression of (a, b) precipitation, (c, d) 850hPa eddy geopotential height and (e, f) 850hPa zonal wind onto (a, c, e) northward period and (b, d, f) peak time precipitation index over East Asia, respectively. Gray dots indicate grids with statistically significant correlation at the 5% significance level. The black rectangle in (a) and (b) represents the northward and peak time precipitation area, respectively. The two black rectangles in (c) and (d) indicate the regions for calculating the western North Pacific subtropical high index. The black rectangles in (e) and (f) indicate the region for calculating the East Asia summer monsoon index

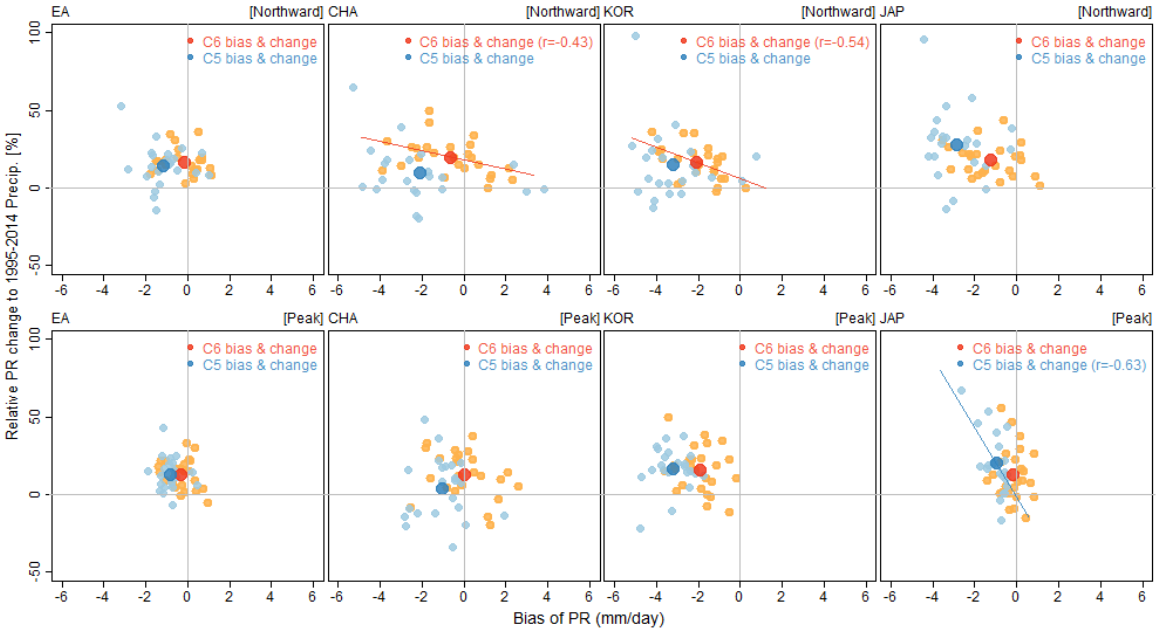

Figure S3. Scatter plot of the association between model biases in precipitation (PR) and its future projections for the long term period (2081–2100) when using the SSP5-8.5 scenario in CMIP6 (orange) and RCP8.5 scenario in CMIP5 (blue). Biases were calculated relative to the observed precipitation data for the 1995–2014 period. Different graphs present the results of models analyzing the Eastern Asian (EA) domain and the subregions of China (CHA), Korea (KOR), and Japan (JAP). Correlation coefficients (r) are provided in case of statistical significant linear regression at the 10% level.

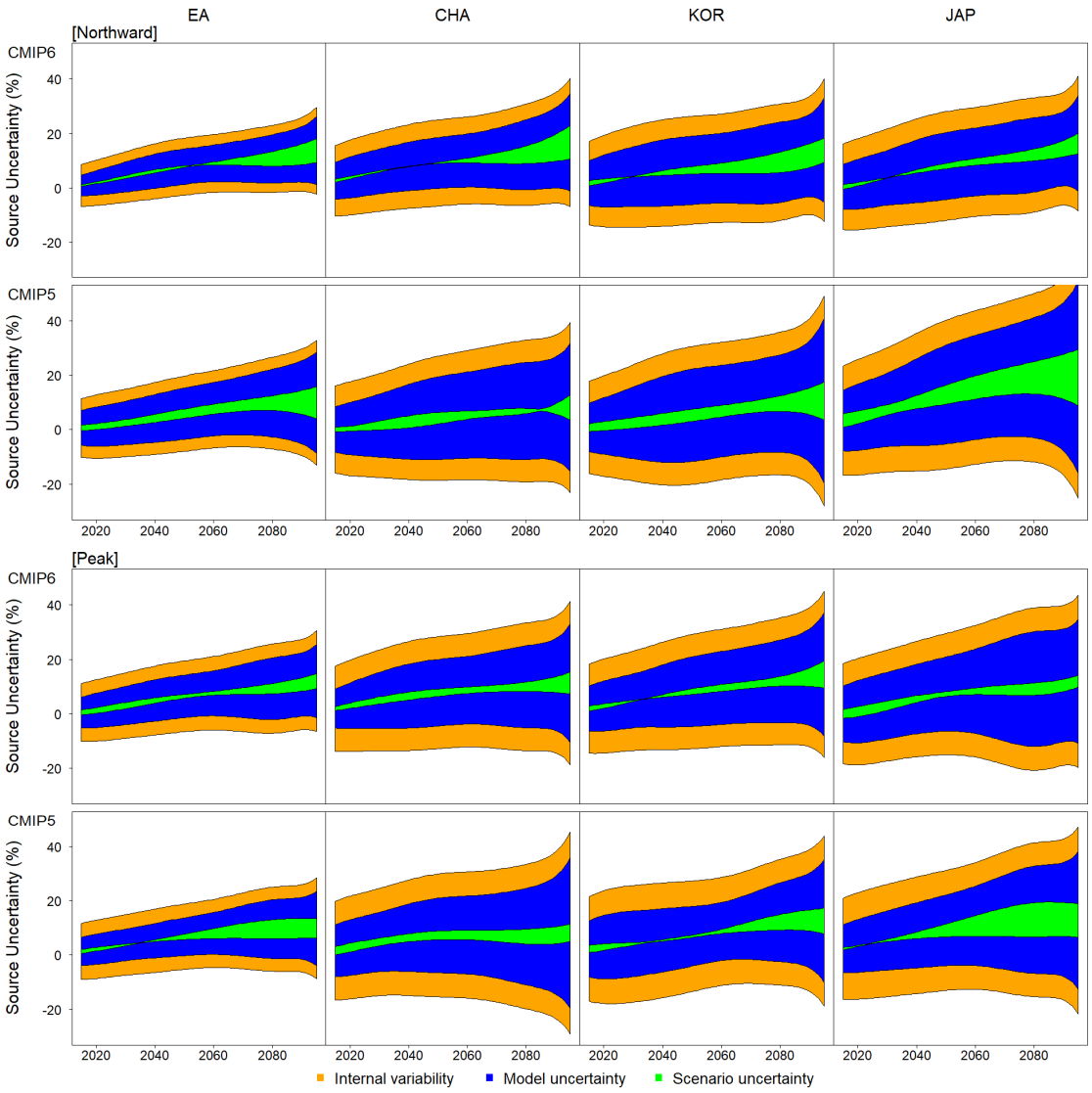

Figure S4. Source of uncertainty in the multi-model multi-scenario mean projection change over East Asia (EA), China (CHA), Korea (KOR), and Japan (JAP) for the northward migration (upper two panels) and the peak time (bottom two panels) of the monsoon band. The top panel in each of these two sets illustrates CMIP6 results, while the bottom panel contains CMIP5 results.

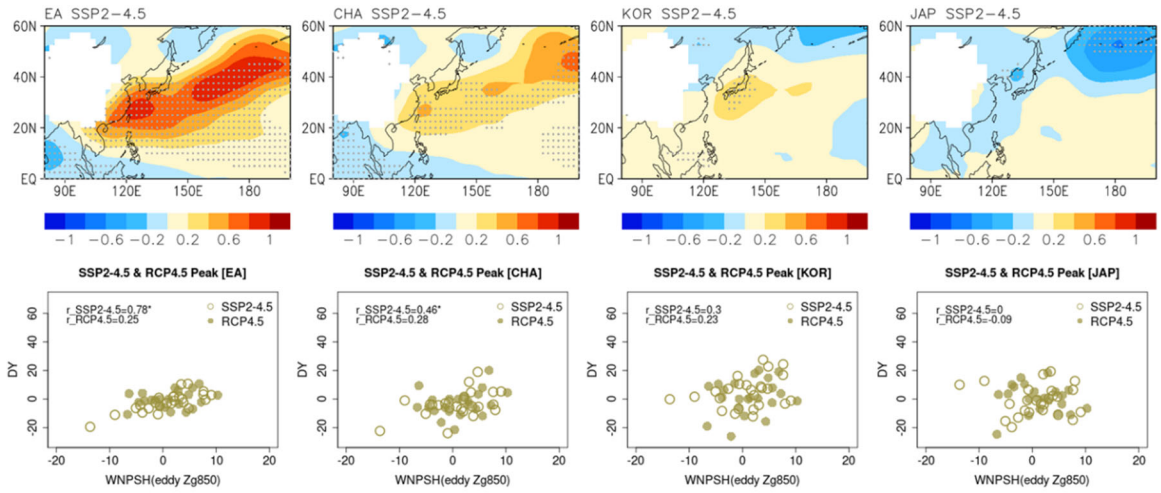

Figure S5. (upper) Inter-model regression of future change 850hPa eddy geopotential height onto the dynamic term of SSP2-4.5 scenario from 25 CMIP6 model for 2081-2100. (bottom) Scatter plot of WNPSH (x-axis) and dynamic term (y-axis) from 25 CMIP6 model (open circle) and 22 CMIP5 model (closed circle). Inter-model correlation is provided and asterisk indicates significant correlation at 5% level.